IEEE Access
Multidisciplinary ⋮ Rapid Review ⋮ Open Access Journal

Received 31 October 2023, accepted 1 December 2023, date of publication 5 December 2023,
date of current version 13 December 2023.

Digital Object Identifier 10.1109/ACCESS.2023.3339559

RESEARCH ARTICLE

Advancement of a High-Efficiency Wearable Antenna Enabling Wireless Body Area Networks

MOHAMED IBRAHIM WALY[1,2], (Member, IEEE), AMOR SMIDA[1,3], (Member, IEEE), NASSER ALI ALJARALLAH[4,5], RIDHA GHAYOULA[3,6], AHMED S. NEGM[7], (Member, IEEE), SURAJO MUHAMMAD[8,9], (Member, IEEE), JUN JIAT TIANG[8], AND AMJAD IQBAL[10,11], (Member, IEEE)

[1]Department of Medical Equipment Technology, College of Applied Medical Sciences, Majmaah University, Al-Majma'ah 11952, Saudi Arabia
[2]Department of Biomedical Engineering and System (formerly), Higher Institute of Engineering, El Shorouk Academy, El Shorouk, Cairo Governorate 11837, Egypt
[3]Microwave Electronics Research Laboratory, Faculty of Mathematical, Physical and Natural Sciences of Tunis, Tunis El Manar University, Tunis 2092, Tunisia
[4]Department of Business Administration, Majmaah University, Al Majma'ah 11952, Saudi Arabia
[5]Health Information Systems Program, AlMaarefa University, Riyadh 13713, Saudi Arabia
[6]Department of Electrical and Computer Engineering, Laval University, Quebec City, QC G1V0A6, Canada
[7]Saudi Consolidated Engineering Company Healthcare Technology Management Administration, King Fahad Medical City, Riyadh 12231, Saudi Arabia
[8]Centre For Wireless Technology (CWT), Faculty of Engineering, Multimedia University, Cyberjaya 63100, Malaysia
[9]Department of Electronics and Telecommunication Engineering, Ahmdu Bello University, Zaria 810211, Nigeria
[10]Institut National de la Recherche Scientifique (INRS), Montreal, QC H5A 1K6, Canada
[11]School of Information Technology (IT), Halmstad University, 301 18 Halmstad, Sweden

Corresponding authors: Mohamed Ibrahim Waly (m.waly@mu.edu.sa), Amor Smida (a.smida@mu.edu.sa), Jun Jiat Tiang (jjtiang@mmu.edu.my), and Amjad Iqbal (aiqbal@ieee.org)

This work was supported by the Deputyship of Research and Innovation, Ministry of Education, Saudi Arabia under Project IFP—2022-06.

ABSTRACT This paper presents a unique antenna that is designed to be efficient, with improved gain and partial flexibility, for use in wearable biomedical telemetry applications. The antenna design utilizes a semi-flexible RO5880 substrate material (dielectric constant, $\varepsilon_r = 2.2$, loss tangent, $(\tan\delta) = 0.0009$) with physical dimensions measuring $0.47\lambda_g \times 0.47\lambda_g$. The model involves the incorporation of rectangular inverted "C" slots, which effectively results in a reduction of the resonant frequency. Additionally, a distributed rectangular slot is introduced on the ground plane, contributing to the augmentation of the operational bandwidth. The operational frequency of the proposed antenna design is 2.40 GHz, accompanied by a bandwidth (BW) of 320 MHz at a −10 dB level. This equates to a fractional percentage bandwidth (FBW) of 13.33% centered around the frequency of 2.40 GHz. The antenna design presented in this work demonstrates the preservation of improved gain and efficiency, achieving values of 3.67 dBi and 94%, respectively, at a frequency of 2.40 GHz. The work demonstrates through simulation and experimental outcomes that the antenna exhibits minimal impact on parameters such as gain reflection coefficient ($|S_{11}|$), BW, and bending efficiency. Furthermore, the antenna underwent simulation and experimental testing in close proximity to the human body, revealing favorable operational characteristics. The proposed antenna exhibits substantial potential as a viable option for wearable biomedical instruments. Thus, the proposed wearable antenna design in this study offers a wideband antenna for ISM band applications, expanding bandwidth without compromising performance. Bending the antenna minimally affects gain, bandwidth, and efficiency when worn on the body, making it suitable for wearables. It also maintains a reasonably low Specific Absorption Rate (SAR), reducing wave absorption by the body. Unique features like rectangular inverted "C" slots and a distributed rectangular slot on the ground plane enhance bandwidth while maintaining performance during bending.

INDEX TERMS Antenna, gain, patch antenna, WBAN applications, SAR, bending condition.

The associate editor coordinating the review of this manuscript and approving it for publication was Eyuphan Bulut.

I. INTRODUCTION

In recent years, there has been a lot of interest in wearable and flexible electronics from both the industrial and academic

sectors [1], [2]. The use of flexible or semi-flexible materials is generating a lot of attention in developing wearable nodes [1]. Flexible electronics can have mechanical behaviors, including wrinkling, bending, and experiencing stress or collapse [3]. These properties would significantly expand the range of applications for current electronic devices, enabling their use in various real-life scenarios that are not flat, including conforming to the shape of the human body [4], [5]. Wireless Body Area Networks (WBANs) find utility in many domains, including sports, security, healthcare, and military applications [6], [7]. These networks can be categorized into three communication modes, each contingent on the location of the signal nodes, specifically on-body, off-body, and in-body modes [8], [9], [10]. For WBAN devices to be effective, they must adhere to critical attributes, including cost-efficiency, low power consumption, high data transmission rates, and the ability to counteract variations in the human body [10], [11]. Hence, the emergence of wearable technology has significantly advanced healthcare, notably in implantable devices [4], [12]. These devices were developed for several medical applications, including neural stimulation [13], cochlear implants [14], pacemakers [15], [16], cardiac defibrillators [17], knee implants [18], [19], bone growth stimulators [20], [21], and foot drop implants [22]. Signals between the implanted device and the wearable network are received and sent by the wearable antenna, which is a key component of the wearable network [23], [24]. The antenna's efficiency should be enhanced because the human body works as a platform that causes electromagnetic (EM) waves to lose energy [25], [26]. Consequently, the body absorbs significant electromagnetic waves and converts them into heat and power [27], [28]. The antenna must be appropriately designed to produce low backward radiations to avoid causing harm to human tissue, commonly known as Specific Absorption Rate (SAR) [29], [30].

Wearable antennas have been developed in a wide variety in recent years [4], [31], [32]. The authors in [29] developed a fractal antenna specifically tailored for 2.4 GHz applications. The antenna has a limited fractional bandwidth (FBW) of 7.75%, and any slight detuning induced by the presence of a human body might result in an impedance mismatch within the intended frequency range. The authors of [33] developed a triangular patch antenna; its operating bandwidth is severely constrained. The authors in [34] construct a small cpw-fed slot antenna for the ISM band applications. On the other hand, the antenna design has a significantly narrow fractional bandwidth of just 6% around its center frequency of 5.83 GHz. There have been various wearable antennas developed, including substrate-integrated waveguide (SIW) based antennas [28], [35], [36] and electromagnetic bandgap (EBG) based antennas [32], [37], [37], all of which have limited bandwidth. The authors in [38] have developed a circularly polarized flexible antenna designed for body-worn applications, operating at 2.4 GHz. The circular polarization of the antenna is attained through the incorporation of edge cuts and side slits in the radiating patch. The substrate is a thicker polyimide spacer, whereas the ground plane and the radiating element comprise nickel-plated fabric.

The authors of [39] demonstrated a wearable antenna design for medical applications using knitted copper as the patch and fabric as the substrate via a ground plane. A T-matching stub is deployed in developing an RFID tag antenna incorporating flexible textile material for UHF application, as described by the authors in [40]. However, the antenna's total size in [39] and [40] makes it impractical for usage in confined system-in-package (SOP) systems. A low-profile wearable button antenna for WLAN applications with an omnidirectional radiation pattern is developed by the authors in [41], employing a flexible Velcro material as a substrate and various reduction methods. The authors in [42] introduced an ISM band wearable antenna, utilizing indigo jeans as the substrate, comprising a rectangular ground plane and a circular patch. A CPW flexible antenna, using a poly-dimethylsiloxane substrate employing a combination of graphene and carbon nanotubes, is designed by the authors in [43] for ISM band applications. Maintaining the antenna performance within an acceptable range while reducing the size of wearable antennas is challenging. Various efforts have been undertaken to decrease the dimensions of the wearable antenna. These attempts, among other techniques, include elongating the resonator length to amplify the current pathway [44], implementing quarter mode designs [28], utilizing high permittivity materials [45], incorporating reactive loading [46], and employing shorting pins [47]. The utilization of the mentioned techniques leads to a considerable decrease in the antenna dimensions. Nonetheless, implementing these techniques introduces other challenges, comprising suboptimal efficiency, limited frequency ranges, and complex configurations. Similarly, the current communication system architecture needs a streamlined structure utilizing uncomplicated design techniques. The procedure of designing an antenna with these features is challenging. Another issue with wearable antennas is the absorption of waves by the human body. The degree to which human tissue absorbs power is illustrated using SAR. Several techniques have been employed in the development of antennas to decrease the SAR ratio, as reported by the authors in [37] and [35], and [48], [49], [50], [51], [52], [53]. The placement of a PEC between the antenna and the human body reduces SAR and improves efficiency, as reported by the authors in [48]. As described by the authors in [49], the SAR value is lowered by adding a ferrite sheet between the antenna and the human body. Using a ferrite sheet lowers signal emission in the opposite direction (backward radiation) with minimal effect on the remaining antenna characteristics. The SAR is reduced by employing a metamaterial structure positioned between the antenna and the human tissue, as demonstrated by the authors in [35], [37], [50], [51], and [52].

This paper presents the design of a 2.4 GHz wideband wearable antenna. The key benefits of this antenna can be summarized as follows:

TABLE 1. Parameters of the proposed wearable antenna.

Parameters	L_g	L_{g1}	L_{g2}	W	L	a	W_f	g
Value (mm)	15	14	7	40	40	35	1.20	2
Parameters	W_{f1}	f	$f1$	$a2$	$a3$	b	$b1$	
Value (mm)	6	5.50	17.80	20	2	15.50	9	

- To the best of our knowledge, this paper introduces a 2.40 GHz wideband wearable antenna that offers a broad operational and fractional bandwidth with a −10 dB level for ISM band application.
- The bending procedures do not significantly impact the acceptable performance of the proposed antenna in terms of gain, operating bandwidth, and efficiency.
- When worn on the body, the antenna demonstrates good bandwidth, positive gain, and improved efficiency. Additionally, when the antenna is positioned on the human body, it maintains a reasonably low SAR value.

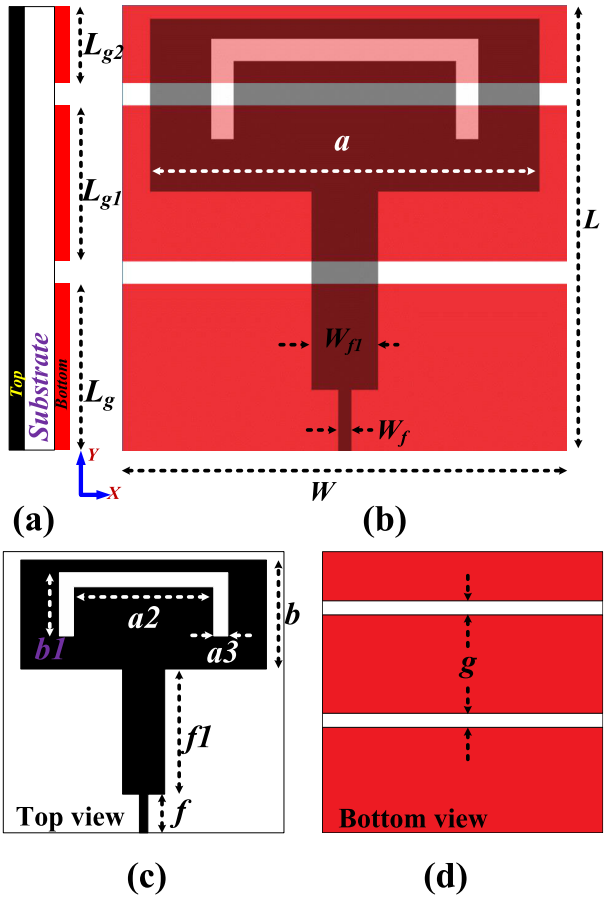

FIGURE 1. Geometry of the proposed wearable antenna portraying the: (a) side view (b) top and bottom view (c) top view and (d) bottom view (All unit are in mm.)

II. ANTENNA DESIGN

The side, perspective, top, and bottom views of the proposed wideband wearable antenna are depicted in Figure. (1a - 1d), respectively. Table. 1, also shows the parameters of the proposed wearable antenna. The substrate utilized is a 1.575 mm thick RT/duroid 5880 semi-flexible material, characterized by its properties ($\varepsilon_r = 2.22$ and $\tan\delta = 0.0009$). A distributed partial ground plane supports a 50 Ω transmission line to excite the radiating element. The antenna's total size measures 40 × 40 × 1.575 mm^3 (equivalent to $0.47\lambda_g \times 0.47\lambda_g \times 0.02\lambda_g$ electrical length). The preliminary radiator measurements were computed using standard formulae for the microstrip patch [54]. The proposed antenna is a redesigned conventional rectangular patch antenna model. The antenna's geometry is reconfigured, and impedance matching at the required operating frequency (f_o) is enhanced by adjusting the ground plane in distributed form and adding inverted "C" slots in the primary radiator. This adjustment and addition are made with less compromise in the gain of the proposed antenna. The antenna's surface current distribution (J_surf), at 2.40 GHz, is shown in Figure. 2.

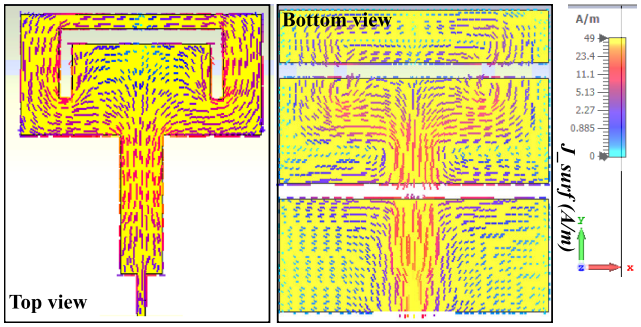

FIGURE 2. Characterization of the antenna's surface current distribution at 2.40 GHz.

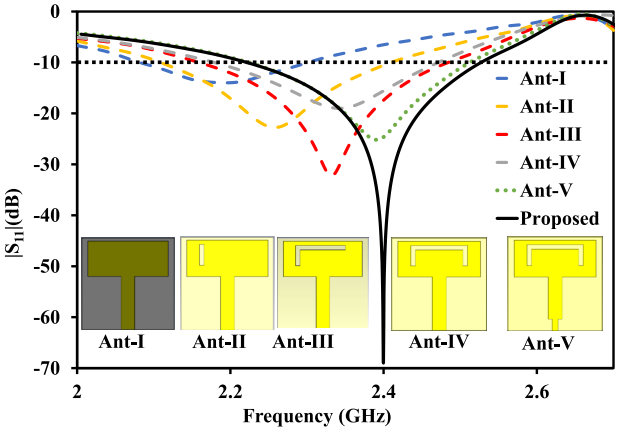

FIGURE 3. Patch design iterative development stages and their respective reflection coefficients ($|S_{11}|$) for the proposed wearable antenna.

A. DESIGN TRANSFORMATION

Figure. 3 depicts the graph of the reflection coefficient ($|S_{11}|$) alongside the design development steps for the patch. The design procedure's initial phase involved utilizing a conventional patch antenna with a rectangular shape. In the initial version (Ant-I), the antenna exhibited a resonance approximately at 2.20 GHz; however, it was not adequately aligned with the desired frequency. The Ant-I underwent

modifications and transformed into Ant-II. A portion of the patch's upper region was etched through a vertical rectangular slot to improve impedance matching at the target frequency. The antenna in Ant-II demonstrated resonance at a frequency of 2.26 GHz, exhibiting a fractional bandwidth (FBW) of 12.85% spanning from 2.11 to 2.40 GHz. In Ant-III, an additional enhancement was made to the antenna design by elongating a rectangular slot on the patch's upper side. In Ant-III, an additional enhancement was made to the antenna design by elongating a rectangular slot on the patch's upper side to 29 mm ($\lambda/3$ at $f_0 = 2.33$). Ant-III exhibited resonance at a frequency of 2.33 GHz, providing a −10 dB bandwidth spanning from 2.17 to 2.48 GHz, corresponding to an FBW of 13.33%. In the Ant-IV examination, the antenna design was further improved by extending a rectangular slot on the upper side of the patch to resemble an inverted ''C'' shape, measuring 38 mm in length (at approximately $\lambda/2$ for $f_0 = 2.40$). Ant-IV demonstrated resonance at a frequency of 2.35 GHz, resulting in a −10 dB bandwidth that covers the range from 2.17 to 2.47 GHz. This corresponds to a fractional bandwidth (FBW) of 12.93%. Modifications were implemented on the Ant-V feedline to achieve the target frequency (step impedance transformer). Two aperture slots measuring 2.4 mm in width were selectively removed from the underside of the feedline. With a bandwidth of −10 dB ranging from 2.22 to 2.52 GHz, Ant-V showed resonance at a frequency of 2.39 GHz. This corresponds to a fractional bandwidth (FBW) of 12.6%.

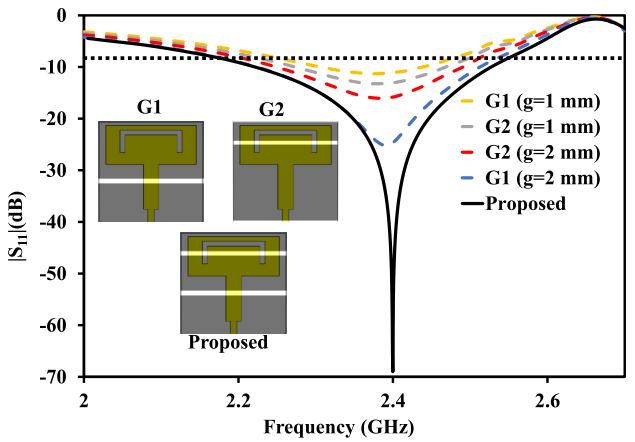

FIGURE 4. Distributed ground design iterative development stages and their respective reflection coefficients ($|S_{11}|$) for the proposed wearable antenna.

B. INFLUENCE OF GROUND PLANE CONFIGURATIONS

The examination of the ground plane involved the utilization of a horizontally distributed rectangular slot, as depicted in Figure. 4. A monopole antenna's resonance relies on the dimensions and placement of the radiating element and the ground plane. The CST full-wave electromagnetic simulator was used to optimize the antenna's ground plane, to improve impedance matching at 2.40 GHz while maintaining a broad impedance bandwidth. Figure. 4 illustrates the influence of diverse ground plane configurations on the antenna, as demonstrated through the $|S_{11}|$ parameter. The antenna exhibits a −10-dB BW from 2.28 to 2.47 GHz, indicating an impedance mismatch, with an average FBW of 8% when employing a conventional partial ground plane configuration (G1 and G2 spaced at 1mm). The antenna demonstrates a bandwidth enhancement at −10 dB observed from 2.22 to 2.52 GHz for the G1 configuration at 2 mm and from 2.25 to 2.50 GHz for the G2 configuration at 2 mm. The average fractional bandwidth achieved is 12.67% for G1 and 10.53% for G2. In this instance, a minimal alteration was observed in the overall gain, although the fractional BW experienced a decrease to 10.53%, as shwon in Figure. 5. The selection of the integrated ground configuration (proposed design) is based on its broad impedance BW and effective impedance matching at the resonant frequency (2.40 GHz). Under Figure. (3 and 4), the proposed design operates at a frequency of 2.40 GHz, surrounding a −10 dB BW spanning from 2.20 to 2.54 GHz. This results in a FBW of 14.30%.

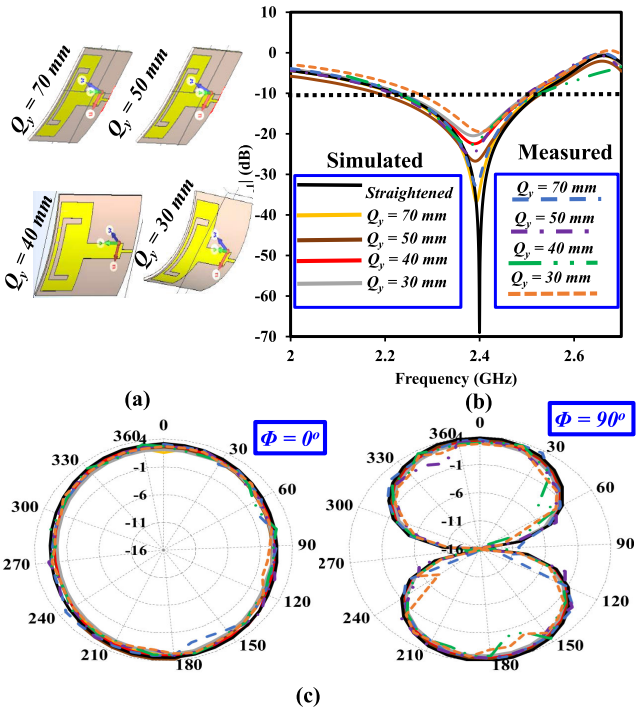

FIGURE 5. (a) Structurally Deformed Antenna with Bending in the *Y − Axis* Direction (Q_y). (b) A comparison between the simulated and measured reflection coefficients ($|S_{11}|$). (c) The respective simulated and measured radiation pattern at 2.40 GHz.

III. INVESTIGATING ANTENNA PERFORMANCE IN WEARABLE APPLICATIONS

This section discusses the suitability of the proposed antenna in scenarios where they are worn on the body. Thus, we investigate the impact of various bending conditions on the performance of a wearable antenna and the level of electromagnetic exposure experienced by the wearer.

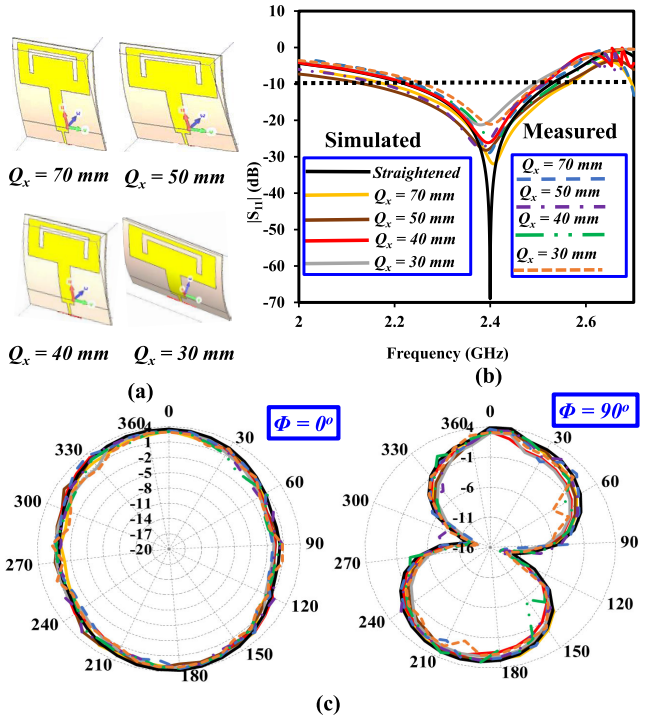

FIGURE 6. (a) Structurally Deformed Antenna with Bending in the $X-Axis$ Direction (Q_x). (b) A comparison between the simulated and measured $|S_{11}|$. (c) The respective simulated and measured radiation pattern at 2.40 GHz.

A. EXAMINING THE MECHANICS OF BENDING

In on-body wearable situations, it is foreseeable that the antenna will undergo bending while actively utilized. This study segment investigates the variations observed in the antenna performance due to bending it in the $x-$ and $y-$ orientations while exposed to free space conditions. To examine the characteristics of the antenna, we opted for different bending radii along the $x-$ and $y-$ directions as, (Q_y and Q_x = [70, 50, 40, and 30 mm]). Our investigation evaluated the antenna's $|S_{11}|$, gain, radiation pattern, and efficiency. The antenna structure is shown in Figure. 5a, demonstrating its response to different bending conditions along the $y-axis$. Figures. 5b and 5c exhibit the antenna's $|S_{11}|$ characteristics and radiation pattern for distinct bending scenarios in the $y-axis$. As easily observed, the resonant frequency experiences an insignificant change for all bending scenarios. Furthermore, it has been observed that the antenna's radiation pattern remains undistorted in both principal planes when operating at 2.4 GHz. Additionally, when the antenna is utilized in bending scenarios, a slight decrease in both its gain and efficiency can be noticed. Also, Figure. 6a illustrates the antenna's configuration at different bending states along the $x-axis$. In Figure. 6b and Figure. 6c, the $|S_{11}|$ parameter and radiation pattern of the antenna are presented for various bending scenarios along the $x-axis$. Evidently, a marginal change in the resonant frequency is observed across all bending scenarios. Also, at 2.4 GHz, the antenna's radiation pattern remains undistorted in both principal planes. Moreover, experimental findings indicate that the antenna's gain and efficiency experience a slight decline when subjected to bending conditions. Both instances demonstrate that the antenna is well-matched at the intended ISM (2.4 GHz) band, albeit with a minor alteration in the resonant frequency. The research demonstrates that the proposed antenna holds potential for utilization in various applications, mainly when the antenna's flexibility is essential. Table. 2 compares and evaluates the antenna's operation under unbent and bent conditions.

TABLE 2. Evaluation of the antenna's operation under unbent and bent conditions.

Bending condition ($y-axis$)					
Q_y (mm)	Straightened	70	50	40	30
Gain (dBi)	3.67	3.42	3.35	3.21	3.01
Efficiency (%)	94.2	92.40	91.23	91.02	90.61
Bending condition ($x-axis$)					
Q_x (mm)	Straightened	70	50	40	30
Gain (dBi)	3.67	3.51	3.23	3.16	3.02
Efficiency (%)	94.2	92.51	92.14	91.73	91.14

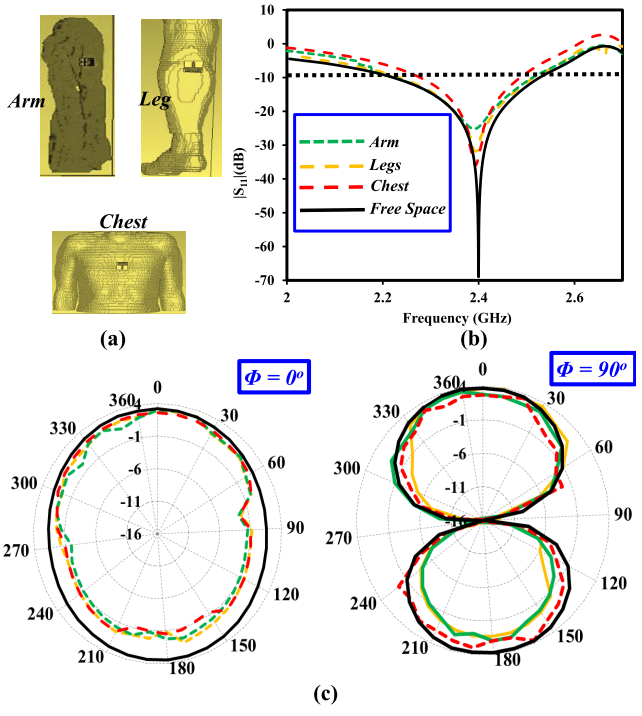

FIGURE 7. (a) Proposed antenna situated on the arm, legs, and chest. (b) The magnitude of the simulated $|S_{11}|$ for each case, and (c) the radiation patterns at 2.40 GHz are shown correspondingly.

B. IMPACT OF LOADING ON THE HUMAN BODY

This section explores the effects of human body loading on the antenna's performance. The antenna's performance was evaluated by loading it on different parts of a lifelike human model, including the arm, chest, and leg, as depicted in Figure. 7a. Figure. 7b depicts the magnitude of the simulated $|S_{11}|$ parameter while situating the antenna on

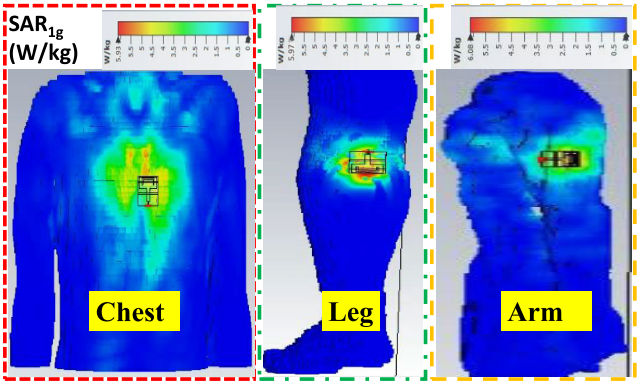

FIGURE 8. The specific absorption rate (SAR_{1g}) of the proposed antenna situated on the chest, leg, and the arm.

TABLE 3. Comparison between free space and on-body worn scenarios.

Parameters	Free Space	Body		
		Arm	Legs	Chest
Resonant Frequency (GHz)	2.40	2.39	2.39	2.39
Bandwidth (%)	13.33	11.25	12.50	8.33
Gain (dBi)	3.67	3.20	3.16	3.23
Efficiency (%)	94.20	81.65	81.22	80.12
SAR_1g (W/kg)	-	6.08	5.97	5.93
VSWR	1.04	1.12	1.15	1.07

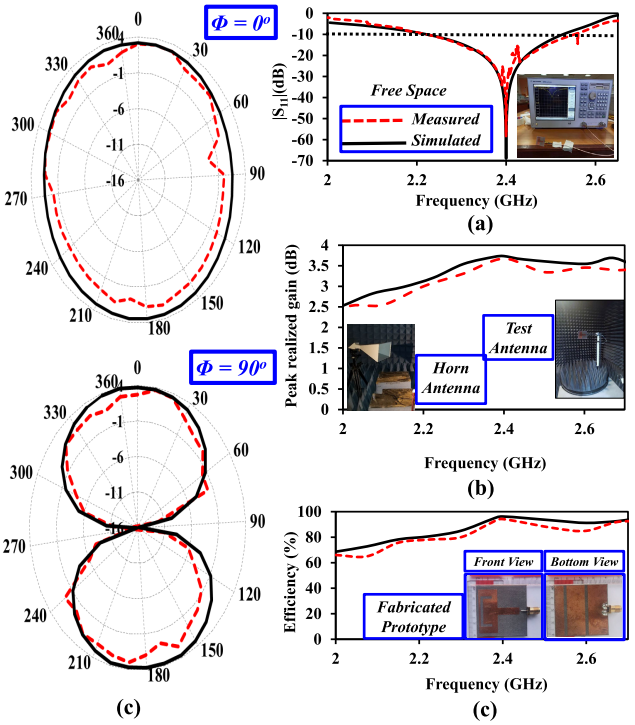

FIGURE 9. Proposed antenna measured (depicted as dashed red line) and simulated (represented as solid black line): (a) $|S_{11}|$ against frequency, (b) peak realized gain versus frequency (c) efficiency versus frequency, and (c) the distribution of radiation pattern at 2.40 GHz.

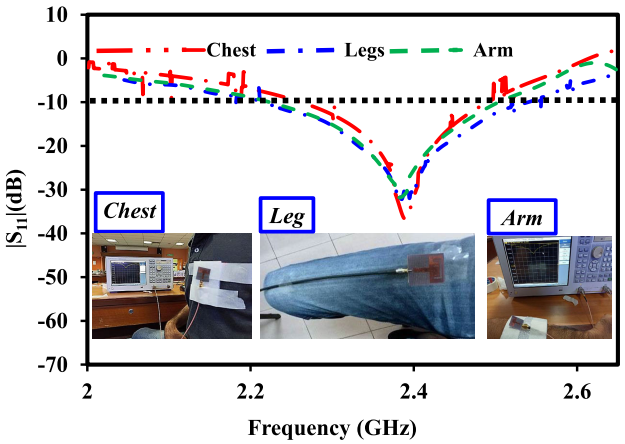

FIGURE 10. The magnitude of the measured $|S_{11}|$ situated on the chest, leg, and the arm of the proposed antenna fabricated prototype.

the arm, chest, and legs. The observed resonant frequency of the loaded antenna was found to be lower than that of the free space antenna. This phenomenon is attributed to the increased permittivity exhibited by the human body. The antenna's resonant frequency occurred at 2.39 GHz (−36 dB), and its fractional bandwidth (FBW) measured 8.33% when positioned on the chest. Upon subjecting the antenna to simulation on legs, a slight alteration in resonant frequency to 2.394 GHz (−25.11 dB) was observed, accompanied by an increased FBW of 12.50%. The antenna placement on the arm revealed that the resonant frequency registered a value of 2.398 GHz (−31.67 dB) while concurrently displaying an FBW of 11.25%. It was observed that the body-loaded antenna exhibited an FBW that is slightly narrower compared to the free-space antenna at 13.33% (−69 dB). Nonetheless, it effectively enveloped the intended ISM band centered at 2.40 GHz. Thus, an insubstantial influence from the loading of the human body was observed on the antenna's radiation pattern, as depicted in Figure. 7c. In scenarios involving on-body wearing, the performance metrics of the antenna, namely its efficiency and gain, experienced degradation. This degradation can be attributed to the inherent absorption characteristics of human muscles, tissues, bones, and related factors. An investigation into the impact of electromagnetic (EM) exposure on the human body, focusing on a specific absorption rate (SAR) at the resonant frequency of 2.40 GHz, was conducted on the proposed antenna. The study was carried out to assess the SAR attributes of the antenna. This evaluation examined the chest, legs, and arm areas as the focal points of interest. A spatial separation of 6 mm was maintained between the antenna and the human body to simulate the SAR scenario. SAR values of 5.93, 5.97, and 6.08 W/kg for the chest, legs, and arm were observed. These SAR measurements were calculated by taking the average across 1 g of tissue, employing an input power of 1 W. Nevertheless, there are restrictions on how much power the devices near the human body can handle [55], [56]. In the context of wearable devices, the antenna design under consideration demonstrates its safety when employed, provided that the incoming power remains below 265 mW. Figure. 8 depicts the SAR simulation conducted on the chest, leg, and arm. Table. 3 presents an overview of the

TABLE 4. Comparative evaluation of performance against existing wearable antennas reported in the literature.

Ref[...]	Dimensions $\lambda_g \times \lambda_g$	Range of Frequencies (GHz)	Efficiency (%)	Gain (dBi)	FBW (%)	Design: Complexity	Substrate: material (Type: ε_r)
[3]	0.52 × 0.33	∼2.27 – 2.56	29.17	1.41	11.84	Medium	Polydimethylsiloxane (Flexible: 2.7)
[4]	0.46 × 0.46	2.36 – 2.55	75	2.06	7.75	Complex	RO5880 (Semi-flexible: 2.2)
[12]	0.46 × 0.46	∼2360 – 2460	74	4.00	4.17	Medium	Wool felt (Semi-flexible: 1.2)
[24]	0.72 × 0.72	2.28 – 2.64	>70	7.3	14.7	Medium	Wool felt (Semi-flexible: 1.2)
[25]	0.63 × 0.63	∼2.30 – 2.50	NA	6.55	8.30	Medium	Denim Jeans (Flexible: 1.7)
[28]	0.58 × 0.58	2.39 – 2.51	81	4.20	4.90	Simple	Textile (Flexible: 1.495)
[30]	0.70 × 0.70 0.85 × 0.85	∼2320 – 2520	NA	2.83	8.26	Complex	Felt & Teflon (Flexible: 1.36&2.1)
[31]	0.57 × 0.61	2.358 – 2.447 5.675 – 5.975	91.4/ 92.3	3.74/ 5.13	3.80/ 5.20	Simple	RO3003 (Semi-flexible: 3)
[32]	1.12 × 1.12	2.40 – 2.50 5.15 – 5.825	NA	3.00/ 4.50	4.00/ 12	Simple	Fabric Textile (Flexible: 1.38)
[35]	0.51 × 0.40	2.43 – 2.45 5.72 – 5.83	91/ 96	1.77/ 3.14	1.20/ 1.90	Complicated	RO5870 (Semi-flexible: 2.33)
[37]	1.56 × 1.56	1.78 –1.98 2.38 – 2.45	NA	10.92/ 5.08	NA	Simple	Jean Fabric (Flexible: 1.7)
This Work	0.47 × 0.47	2.21 – 2.53	94.20	3.67	13.33	Medium	R5880 (Semi-flexible: 2.2)

λ_g: Wavelength at the lowest operating frequency (f_o).
NA: Not available.

proposed antenna performance for free-space and on-body worn situations.

IV. RESULTS AND DISCUSSION

The proposed wearable antenna is fabricated through a semi-flexible substrate material, RO5880. This material possesses an effective relative permittivity (ε_r) value of 2.2 alongside a nominal loss tangent ($\tan\delta$) value of 0.0009. A series of measurements to evaluate the $|S_{11}|$ of the proposed wearable antenna under two conditions: in free space and when worn on the body, is conducted in this work. A vector network analyzer was employed for these measurements. Additionally, we assessed the antenna's radiation pattern in a free-space environment within an anechoic chamber. Figure. 9 visually represents the metrics for the antenna in a free-space environment, including the

measured $|S_{11}|$, efficiency, gain, and radiation pattern. Table. 3 also presents the antenna parameters for the arm, legs, and chest.

In this study, we measured the antenna's on-body $|S_{11}|$ on an individual aged 32 years with a weight of 75 kg and a height of 176.25 cm. The $|S_{11}|$ measurement of the antenna prototype was conducted across various body positions, including the chest, legs, and arm. A layer of Styrofoam was strategically positioned to separate the antenna from the main body. The antenna itself was affixed securely onto the body by applying adhesive tape. The $|S_{11}|$ of the antenna operating within a free space is illustrated in Figure. 9a, showcasing a side-by-side analysis of both simulated and measured outcomes. The outcomes obtained through simulation closely corresponded with the experimental measurements within the operational frequency range. The -10 dB FBW was determined through measurement (simulation) to be 227 MHz (320 MHz), accompanied by a corresponding FBW of 9.58% (13.33%). The measured antenna gain and efficiency were evaluated and contrasted against the simulation outcomes, as depicted in Figure. 9b. Observations indicate a minimal disparity between the outcomes obtained through simulation and the measurements concerning gain and efficiency. The proposed antenna's radiation pattern was investigated along its principal planes ($\phi = 0^o$ and $\phi = 90^o$). The measurements were conducted in an anechoic chamber designed to suppress echoes. A comparison was drawn between the measured data and the simulated results, as illustrated in Figure. 9c. Figure. 10 illustrates the magnitude of the $|S_{11}|$ measurements of the proposed antenna during its placement on various body areas such as the chest, legs, and arm. Observations reveal that the antenna's resonant frequency remains consistently within the operational band of 2.40 GHz across various placement scenarios, including the chest, leg, and arm. Investigation into on-body BW characteristics is carried out at -10 dB. A slight variability in BW performance is explored across distinct anatomical sites, namely the chest, leg, and arm, where the antenna was situated.

The outcome reveals bandwidth measurements of 198, 310, and 280 MHz for the chest, leg, and arm positions. FBW of 8.25%, 12.10%, and 10.83% are documented, elucidating the differing frequency behaviors across these on-body locations. The discrepancy observed between the simulated values enacted on the physical body and the values obtained through measurement is a result of multiple contributing factors, including the dissipation of energy within the SMA connector elements, signal attenuation within the connecting cable mediums, and inherent limitations in the precision of the calibration techniques employed for the measurement devices.

In this study, we present a comparative analysis in Table. 4, highlighting the advantages exhibited by the proposed antenna within the ISM band in contrast to the related available wearable antennas from the literature. The comparative analysis between the proposed wearable antenna design and existing literature focuses on dimensions, operational efficiency, efficiency, gain, FBW, and the material substrate. An analysis of the results reveals that the antenna configuration presented in this research showcases improved dimensional characteristics compared to most comparable counterparts. It is worth noting that a previous study conducted by the authors in [4] accomplished a size reduction. Nevertheless, our proposed antenna design achieves heightened efficiency, gain, and fractional bandwidth (FBW). Consequently, the FBW portrayed by our suggested antenna design outperforms that of related works. It is worth highlighting that, despite the marginal gain and fractional bandwidth enhancement achieved by the authors in [24], our proposed design achieves better efficiency while occupying a smaller spatial footprint. This inherent characteristic renders our proposed antenna configuration particularly amenable to seamless integration into wearable technology applications.

V. CONCLUSION

In this study, we present the development of a wideband antenna tailored for integration into wearable biomedical devices, emphasizing its low-profile design. The reduction in antenna size has been effectively achieved by introducing rectangular inverted "C" slots into the conventional rectangular patch configuration. Additionally, an expansion in bandwidth has been realized through the utilization of a distributed rectangular slot coupled with the ground plane. The fabricated antenna demonstrated resonance at 2.40 GHz, accompanied by a BW of 320 MHz (-10 dB), corresponding to an approximate FBW coverage of 13.33% at 2.40 GHz. The antenna design proposed in this work retained good levels of gain and efficiency when tested in open space conditions and when utilized in a scenario involving attachment to the human body. Furthermore, the antenna exhibits acceptable operational characteristics when bending along the $x - axis$ and $y - axis$. Moreover, the antenna's SAR_{1g} measurement remains within the boundaries delineated by the IEEE, where the recorded value surpasses 1.60 W/kg for an input power lower than 265.0 mW. The proposed antenna exhibits promising attributes as a potential component for wearable biomedical devices due to its small dimensions, improved efficiency, and gain in human-body loading scenarios.

ACKNOWLEDGMENT

The authors are grateful to the co-authors for their encouragement, expertise, and contributions to this work. The funders had no role in study design, data collection and analysis, decision to publish, or preparation of the manuscript.

REFERENCES

[1] F. F. Hashim, W. N. L. B. Mahadi, T. B. A. Latef, and M. B. Othman, "Key factors in the implementation of wearable antennas for WBNs and ISM applications: A review WBNs and ISM applications: A review," *Electronics*, vol. 11, no. 15, p. 2470, Aug. 2022.

[2] K. Zhang, G. A. E. Vandenbosch, and S. Yan, "A novel design approach for compact wearable antennas based on metasurfaces," *IEEE Trans. Biomed. Circuits Syst.*, vol. 14, no. 4, pp. 918–927, Aug. 2020.

[3] G. S. Latha, G. S. N. Raju, and P. A. Sunny Dayal, "Design and analysis metamaterial inspired wearable antenna for 2.45 GHz ISM band," in *Proc. 32nd Int. Conf. Microelectron. (ICM)*, Dec. 2020, pp. 1–4.

[4] A. Arif, M. Zubair, M. Ali, M. U. Khan, and M. Q. Mehmood, "A compact, low-profile fractal antenna for wearable on-body WBAN applications," *IEEE Antennas Wireless Propag. Lett.*, vol. 18, no. 5, pp. 981–985, May 2019.

[5] C. Hou, H. Wang, and G. Wang, *Flexible and Wearable Electronics for Smart Clothing*. Hoboken, NJ, USA: Wiley, 2020.

[6] H. Yalduz, T. E. Tabaru, V. T. Kilic, and M. Turkmen, "Design and analysis of low profile and low SAR full-textile UWB wearable antenna with metamaterial for WBAN applications," *AEU-Int. J. Electron. Commun.*, vol. 126, Nov. 2020, Art. no. 153465.

[7] S. Muhammad, M. I. Waly, N. A. AlJarallah, R. Ghayoula, A. S. Negm, A. Smida, A. Iqbal, J. J. Tiang, and M. Roslee, "A multiband SSr diode RF rectifier with an improved frequency ratio for biomedical wireless applications," *Sci. Rep.*, vol. 13, no. 1, p. 13246, Aug. 2023.

[8] G.-P. Gao, Z.-H. Dou, Z.-Q. Yu, B.-K. Zhang, J.-H. Dong, and B. Hu, "Dual-mode patch antenna with capacitive coupling structure for on-/off-body applications," *IEEE Antennas Wireless Propag. Lett.*, vol. 21, no. 8, pp. 1512–1516, Aug. 2022.

[9] N. Ziaei and A. Avokh, "Relay selection, clustering, and data aggregation routing in wireless body area networks," *Int. J. Commun. Syst.*, vol. 34, no. 10, p. e4837, Jul. 2021.

[10] S. Muhammad, J. J. Tiang, M. Roslee, M. I. Waly, N. K. Mallat, A. Smida, and A. Iqbal, "Advancing IoT wireless sensor nodes with a low profile multiband RF rectifier based on multi-stub J-inverter network," *AEU-Int. J. Electron. Commun.*, vol. 171, Nov. 2023, Art. no. 154869.

[11] C. Mao, P. L. Werner, D. H. Werner, D. Vital, and S. Bhardwaj, "Dual-polarized armband embroidered textile antenna for on-/off-body wearable applications," in *Proc. IEEE Int. Symp. Antennas Propag. USNC-URSI Radio Sci. Meeting*, Jul. 2019, pp. 1555–1556.

[12] M. Wagih, G. S. Hilton, A. S. Weddell, and S. Beeby, "Dual-polarized wearable antenna/rectenna for full-duplex and MIMO simultaneous wireless information and power transfer (SWIPT)," *IEEE Open J. Antennas Propag.*, vol. 2, pp. 844–857, 2021.

[13] Y. U. Cho, S. L. Lim, J.-H. Hong, and K. J. Yu, "Transparent neural implantable devices: A comprehensive review of challenges and progress," *Npj Flexible Electron.*, vol. 6, no. 1, p. 53, Jun. 2022.

[14] M. Yip, R. Jin, H. H. Nakajima, K. M. Stankovic, and A. P. Chandrakasan, "A fully-implantable cochlear implant SoC with piezoelectric middle-ear sensor and arbitrary waveform neural stimulation," *IEEE J. Solid-State Circuits*, vol. 50, no. 1, pp. 214–229, Jan. 2015.

[15] S. J. Seidman, J. Guag, B. Beard, and Z. Arp, "Static magnetic field measurements of smart phones and watches and applicability to triggering magnet modes in implantable pacemakers and implantable cardioverter-defibrillators," *Heart Rhythm*, vol. 18, no. 10, pp. 1741–1744, Oct. 2021.

[16] S. M. Asif, A. Iftikhar, J. W. Hansen, M. S. Khan, D. L. Ewert, and B. D. Braaten, "A novel RF-powered wireless pacing via a rectenna-based pacemaker and a wearable transmit-antenna array," *IEEE Access*, vol. 7, pp. 1139–1148, 2019.

[17] U. Rohrer, M. Manninger, A. Zirlik, and D. Scherr, "Multiparameter monitoring with a wearable cardioverter defibrillator," *Sensors*, vol. 22, no. 1, p. 22, Dec. 2021.

[18] M. Jain, M. Stanacevic, R. Willing, S. Towfighian, and E. Salman, "Wireless power transfer for smart knee implants," in *Proc. IEEE Int. Symp. Circuits Syst. (ISCAS)*, May 2022, pp. 1896–1900.

[19] E. Kelmers, A. Szuba, S. W. King, J. Palan, S. Freear, H. G. Pandit, and B. H. van Duren, "Smart knee implants: An overview of current technologies and future possibilities," *Indian J. Orthopaedics*, vol. 57, no. 5, pp. 635–642, 2022.

[20] I. Peres, P. Rolo, and M. P. Soares Dos Santos, "Multifunctional smart bone implants: Fiction or future?—A new perspective," *Frontiers Bioeng. Biotechnol.*, vol. 10, p. 926, Jun. 2022.

[21] L. Leppik, K. M. C. Oliveira, M. B. Bhavsar, and J. H. Barker, "Electrical stimulation in bone tissue engineering treatments," *Eur. J. Trauma Emergency Surg.*, vol. 46, no. 2, pp. 231–244, Apr. 2020.

[22] D. J. Weber, R. B. Stein, K. M. Chan, G. Loeb, F. Richmond, R. Rolf, K. James, and S. L. Chong, "BIONic WalkAide for correcting foot drop," *IEEE Trans. Neural Syst. Rehabil. Eng.*, vol. 13, no. 2, pp. 242–246, Jun. 2005.

[23] A. Alemaryeen and S. Noghanian, "On-body low-profile textile antenna with artificial magnetic conductor," *IEEE Trans. Antennas Propag.*, vol. 67, no. 6, pp. 3649–3656, Jun. 2019.

[24] G.-P. Gao, B. Hu, S.-F. Wang, and C. Yang, "Wearable circular ring slot antenna with EBG structure for wireless body area network," *IEEE Antennas Wireless Propag. Lett.*, vol. 17, no. 3, pp. 434–437, Mar. 2018.

[25] A. Y. I. Ashyap, Z. Z. Abidin, S. H. Dahlan, H. A. Majid, M. R. Kamarudin, A. Alomainy, R. A. Abd-Alhameed, J. S. Kosha, and J. M. Noras, "Highly efficient wearable CPW antenna enabled by EBG-FSS structure for medical body area network applications," *IEEE Access*, vol. 6, pp. 77529–77541, 2018.

[26] C. Lim, Y. Shin, J. Jung, J. H. Kim, S. Lee, and D.-H. Kim, "Stretchable conductive nanocomposite based on alginate hydrogel and silver nanowires for wearable electronics," *APL Mater.*, vol. 7, no. 3, Mar. 2019, Art. no. 031502.

[27] S. Bakogianni and S. Koulouridis, "A dual-band implantable rectenna for wireless data and power support at sub-GHz region," *IEEE Trans. Antennas Propag.*, vol. 67, no. 11, pp. 6800–6810, Nov. 2019.

[28] S. Agneessens, S. Lemey, T. Vervust, and H. Rogier, "Wearable, small, and robust: The circular quarter-mode textile antenna," *IEEE Antennas Wireless Propag. Lett.*, vol. 14, pp. 1482–1485, 2015.

[29] A. Bouazizi, G. Zaibi, A. Iqbal, A. Basir, M. Samet, and A. Kachouri, "A dual-band case-printed planar inverted-F antenna design with independent resonance control for wearable short range telemetric systems," *Int. J. RF Microw. Comput.-Aided Eng.*, vol. 29, no. 8, Aug. 2019, Art. no. e21781.

[30] A. B. Mustafa and T. Rajendran, "An effective design of wearable antenna with double flexible substrates and defected ground structure for healthcare monitoring system," *J. Med. Syst.*, vol. 43, no. 7, pp. 1–11, Jul. 2019.

[31] U. Musa, S. M. Shah, H. A. Majid, I. A. Mahadi, M. K. A. Rahim, M. S. Yahya, and Z. Z. Abidin, "Design and analysis of a compact dual-band wearable antenna for WBAN applications," *IEEE Access*, vol. 11, pp. 30996–31009, 2023.

[32] S. Zhu and R. Langley, "Dual-band wearable textile antenna on an EBG substrate," *IEEE Trans. Antennas Propag.*, vol. 57, no. 4, pp. 926–935, Apr. 2009.

[33] C. Mohan and S. E. Florence, "Miniaturised triangular microstrip antenna with metamaterial for wireless sensor node applications," *IETE J. Res.*, vol. 68, no. 2, pp. 1177–1182, Mar. 2022.

[34] Y. J. Li, Z. Y. Lu, and L. S. Yang, "CPW-fed slot antenna for medical wearable applications," *IEEE Access*, vol. 7, pp. 42107–42112, 2019.

[35] X.-Q. Zhu, Y.-X. Guo, and W. Wu, "A compact dual-band antenna for wireless body-area network applications," *IEEE Antennas Wireless Propag. Lett.*, vol. 15, pp. 98–101, 2016.

[36] S. Agneessens and H. Rogier, "Compact half diamond dual-band textile HMSIW on-body antenna," *IEEE Trans. Antennas Propag.*, vol. 62, no. 5, pp. 2374–2381, May 2014.

[37] S. Velan, E. F. Sundarsingh, M. Kanagasabai, A. K. Sarma, C. Raviteja, R. Sivasamy, and J. K. Pakkathillam, "Dual-band EBG integrated monopole antenna deploying fractal geometry for wearable applications," *IEEE Antennas Wireless Propag. Lett.*, vol. 14, pp. 249–252, 2015.

[38] M. Klemm, I. Locher, and G. Troster, "A novel circularly polarized textile antenna for wearable applications," in *Proc. 7th Eur. Conf. Wireless Technol.*, 2004, pp. 285–288.

[39] P. Salonen and L. Hurme, "A novel fabric WLAN antenna for wearable applications," in *IEEE Antennas Propag. Soc. Int. Symp. Dig. Held Conjunct, USNC/CNC/URSI North Amer. Radio Sci. Meeting*, Jun. 2003, pp. 700–703.

[40] Y.-H. Kim and Y.-C. Chung, "UHF RFID dipole tag antenna design using flexible electro-thread," *J. Korean Inst. Electromagn. Eng. Sci.*, vol. 19, no. 1, pp. 1–6, Jan. 2008.

[41] B. Sanz-Izquierdo, F. Huang, and J. C. Batchelor, "Small size wearable button antenna," in *Proc. 1st Eur. Conf. Antennas Propag.*, Nov. 2006, pp. 1–4.

[42] S. Sankaralingam and B. Gupta, "A circular disk microstrip WLAN antenna for wearable applications," in *Proc. Annu. IEEE India Conf.*, 2009, pp. 1–4.

[43] M. M. Mansor, S. K. A. Rahim, and U. Hashim, "A CPW-fed 2.45 GHz wearable antenna using conductive nanomaterials for on-body applications," in *Proc. IEEE REGION Symp.*, Apr. 2014, pp. 240–243.

[44] C. Liu, Y.-X. Guo, and S. Xiao, "Capacitively loaded circularly polarized implantable patch antenna for ISM band biomedical applications," *IEEE Trans. Antennas Propag.*, vol. 62, no. 5, pp. 2407–2417, May 2014.

[45] J. Kula, D. Psychoudakis, W.-J. Liao, C.-C. Chen, J. Volakis, and J. Halloran, "Patch-antenna miniaturization using recently available ceramic substrates," *IEEE Antennas Propag. Mag.*, vol. 48, no. 6, pp. 13–20, Dec. 2006.
[46] A. P. Saghati, J. S. Batra, J. Kameoka, and K. Entesari, "Miniature and reconfigurable CPW folded slot antennas employing liquid-metal capacitive loading," *IEEE Trans. Antennas Propag.*, vol. 63, no. 9, pp. 3798–3807, Sep. 2015.
[47] H. Wong, K. K. So, K. B. Ng, K. M. Luk, C. H. Chan, and Q. Xue, "Virtually shorted patch antenna for circular polarization," *IEEE Antennas Wireless Propag. Lett.*, vol. 9, pp. 1213–1216, 2010.
[48] A. Hirata, T. Adachi, and T. Shiozawa, "Folded-loop antenna with a reflector for mobile handsets at 2.0 GHz," *Microw. Opt. Technol. Lett.*, vol. 40, no. 4, pp. 272–275, Feb. 2004.
[49] J. Wang and O. Fujiwara, "Reduction of electromagnetic absorption in the human head for portable telephones by a ferrite sheet attachment," *IEICE Trans. Commun.*, vol. 80, no. 12, pp. 1810–1815, 1997.
[50] K. Agarwal, Y.-X. Guo, and B. Salam, "Wearable AMC backed near-endfire antenna for on-body communications on latex substrate," *IEEE Trans. Compon., Packag., Manuf. Technol.*, vol. 6, no. 3, pp. 346–358, Mar. 2016.
[51] Z. H. Jiang, Z. Cui, T. Yue, Y. Zhu, and D. H. Werner, "Compact, highly efficient, and fully flexible circularly polarized antenna enabled by silver nanowires for wireless body-area networks," *IEEE Trans. Biomed. Circuits Syst.*, vol. 11, no. 4, pp. 920–932, Aug. 2017.
[52] P. Prakash, M. P. Abegaonkar, A. Basu, and S. K. Koul, "Gain enhancement of a CPW-fed monopole antenna using polarization-insensitive AMC structure," *IEEE Antennas Wireless Propag. Lett.*, vol. 12, pp. 1315–1318, 2013.
[53] A. Iqbal, A. Basir, A. Smida, N. K. Mallat, I. Elfergani, J. Rodriguez, and S. Kim, "Electromagnetic bandgap backed millimeter-wave MIMO antenna for wearable applications," *IEEE Access*, vol. 7, pp. 111135–111144, 2019.
[54] S. Muhammad, I. Ya'u, A. Abubakar, and A. S. Yaro, "Design of single feed dual-band millimeter wave antenna for future 5G wireless applications," *Sci. World J.*, vol. 14, no. 1, pp. 84–87, 2019.
[55] C. Zebiri, D. Sayad, I. Elfergani, A. Iqbal, W. F. Mshwat, J. Kosha, J. Rodriguez, and R. Abd-Alhameed, "A compact semi-circular and arc-shaped slot antenna for heterogeneous RF front-ends," *Electronics*, vol. 8, no. 10, p. 1123, Oct. 2019.
[56] A. Iqbal, A. Smida, L. F. Abdulrazak, O. A. Saraereh, N. K. Mallat, I. Elfergani, and S. Kim, "Low-profile frequency reconfigurable antenna for heterogeneous wireless systems," *Electronics*, vol. 8, no. 9, p. 976, Aug. 2019.

MOHAMED IBRAHIM WALY (Member, IEEE) received the degree in biomedical engineering and system baccalaureate, the M.Sc. degree in biomedical engineering and system, and the Ph.D. degree from the Faculty of Biomedical Engineering and System, Cairo University, in 2004, 2009, and 2013, respectively. From 2004 to 2015, he was a Consultant Engineer with CASBEC, from 2013 to 2015. Since October 2015, he has been an Assistant Professor with the Department of Medical Equipment Technology, College of Applied Medical Sciences, Majmaah University, Saudi Arabia. His current research interests include design microwave antennas for biomedical applications, machine learning applications in medical field, predication disease model, system dynamic model, and clinical engineering management systems.

AMOR SMIDA (Member, IEEE) received the degree in electronic baccalaureate, the M.Sc. degree in analyze and digital processing of the electronic systems, and the Ph.D. degree from the Faculty of Mathematical, Physical and Natural Sciences of Tunis, Tunis El-Manar University, Tunisia, in 2008, 2010, and 2014, respectively. From 2008 to 2014, he was a Graduate Student Researcher with the Unit of Research in High Frequency Electronic Circuits and Systems. Since August 2014, he has been an Assistant Professor with the Department of Medical Equipment Technology, College of Applied Medical Sciences, Majmaah University, Saudi Arabia. His current research interests include smart antennas, biosensors, biomedical applications, neural network applications in antennas, adaptive arrays, and microwave circuits design CST studio microwave.

NASSER ALI ALJARALLAH received the bachelor's degree in health services administration and the master's degree in health and hospital administration from King Saud University, and the Ph.D. degree in business administration from the University of Hull, U.K. He is currently a Vice Rector of AlMaarefa University, an Assistant Professor of Quality Management with the College of Business Administration, Majmaah University, and the Chairperson of the Scientific Committee with the Saudi Society for Health Administration. He has participated and consulted in various sectors. His research interests include quality and entrepreneurship. He is a member of five teams of patent inventors and won four gold medal.

RIDHA GHAYOULA received the Dipl. Eng. degree in electrical engineering and the M.Sc. degree in analyze and digital processing of the electronic systems, in 2002 and 2005, respectively, and the Ph.D. degree from the Faculty of Mathematical, Physical, and Natural Sciences of Tunis, Tunis El-Manar University, Tunisia, in 2008. From 2004 to 2012, he was a Graduate Student Researcher with the Unit of Research in High Frequency Electronic Circuits and Systems. He has worked on several industrial experiences in Canada as an FPGA Designer, in 2014, with Aerostar Research and Development, Doric Lenses Inc., in 2017, Telops Inc., in 2018, and M2S Electronics, Canada, in 2019. Since August 2009, he has been an Assistant Professor with the Electrical Engineering Department, Higher Institute of Computer Science of El Manar, Tunisia, and an Associate Professor, from 2014 to 2015. Since May 2012, he has been a Postdoctoral Fellow with LRTS, Department of Electrical and Computer Engineering, Laval University, Quebec, QC, Canada. His current research interests include software engineering, FPGA, softcore processor, modeling and simulation, TDOA, DOA, phased arrays, smart antennas, direction finding, radio-communication systems, neural network applications in antennas, adaptive arrays, and microwave circuits design. He has published more than 75 journals and conference papers on smart antennas and embedded systems. He has participated in several industrial projects in North America for five years in the embedded field, real time, LidAR, and FPGA, for example, Dual optogenetic stimulation with a Laser Diode Fiber Light Source, Hyperspectral IR Cameras, DE-8209 ORKAN-UP15 (C0069A), HVAC Application: TNG15-TX070, and HVAC Application: DE-8209 TOUCH18 WiFi-TX120.

AHMED S. NEGM (Member, IEEE) received the B.Sc. degree in system and biomedical engineering from the Higher Institute of Engineering, Shorouk Academy, in 2000, the degree in medical imaging (decision support system for lymphoma classification), in 2009, the master's degree in system and biomedical engineering from the System and Biomedical Engineering Department, Faculty of Engineering, Cairo University, in 2017, the Doctor of Philosophy degree in system and biomedical engineering from the System and Biomedical Engineering Department, Faculty of Engineering, Cairo University, and the degree in medical imaging (automatic segmentation and classification of acute leukemia cells in microscopic images). He is currently a Healthcare Technology Management Administration Consultant. His current research interests include design microwave antennas for biomedical applications, machine learning applications in medical field, predication disease model, system dynamic model, and clinical engineering management systems.

SURAJO MUHAMMAD (Member, IEEE) received the B.Eng. degree in computer engineering from Bayero University, Kano, Nigeria, in 2004, the M.Eng. degree in electronics and telecommunications engineering from the Universiti of Teknologi, Johor, Malaysia, in 2014, and the Ph.D. degree from the Faculty of Engineering, Multimedia University, Cyberjaya, Selangor, Malaysia, in 2022. Currently, he is a Lecturer-I with the Department of Electronics and Telecommunication Engineering (ETEND), Ahmdu Bello University (ABU), Zaria, Nigeria, and a Postdoctoral Researcher with Multimedia University. His research interests include RF energy harvesting (RFEH) for biomedical implants, wireless power transfer systems for biomedical implants, 5G mm-wave antennas, and wearable and implantable antennas.

JUN JIAT TIANG received the degree in electronics engineering from Multimedia University, Malaysia, the master's degree from the University of Science, Malaysia, and the Ph.D. degree from Universiti Kebangsaan Malaysia (UKM). He was a Design Automation Engineer with the Chipset Structural Design Team, Intel Microelectronics (M) Sdn. Bhd., Penang, Malaysia, from September 2004 to July 2005, and an Electronics Engineer with the Global Technology Development Group, Motorola Technology Sdn. Bhd., Penang, from May 2006 to May 2007. He has vast experience while working as the Project Leader in various research grants, such as TM Research and Development, from 2017 to 2020; Research Grant, Ministry of Science, Technology and Innovation (MOSTI), from 2008 to 2010; and research grant Mini Fund, in 2016. He is currently a Senior Lecturer and a Researcher with the Faculty of Engineering, Multimedia University. His research interests include RFID, microwave circuits, antenna, and propagation. He was awarded the Gold Medal at the 23rd International Invention, Innovation, and Technology Exhibition (ITEX) 2012, Kuala Lumpur, Malaysia, in May 2012, and the Silver Medal at the Malaysian Technology Expo (MTE) 2013, Kuala Lumpur, in February 2013.

AMJAD IQBAL (Member, IEEE) received the degree in electrical engineering from COMSATS University, Islamabad, Pakistan, in 2012, the master's degree in electrical engineering from the Department of Electrical Engineering, CECOS University of IT and Emerging Science, Peshawar, Pakistan, in 2018, and the Ph.D. degree from the Faculty of Engineering, Multimedia University, Cyberjaya, Selangor, Malaysia. He was a Laboratory Engineer with the Department of Electrical Engineering, CECOS University, Peshawar, from 2016 to 2018. His research interests include printed antennas, flexible antennas, implantable antennas, MIMO antennas, dielectric resonator antennas, and the synthesis of microwave components.